Light-fields of Circular Camera Arrays

Aron Cserkaszky*, Peter A. Kara†, Attila Barsi*, Maria G. Martini† and Tibor Balogh*
*Holografika, Budapest, Hungary
Email: {a.cserkaszky, a.barsi, t.balogh}@holografika.com
†WMN Research Group, Kingston University, UK
Email: {p.kara, m.martini}@kingston.ac.uk

***Abstract*—The ray structure and sampling properties of different light-field representations inherently determine their use-cases. Currently prevalent linear data structures do not allow for joint processing of light-fields captured from multiple sides of a scene. In this paper, we review and highlight the differences in capturing and reconstruction between light-fields captured with linear and circular camera arrays. We also examine and improve the processing of light-fields captured with circular camera arrays with a focus on their use in reconstructing dense light-fields, by proposing a new resampling technique for circular light-fields. The proposed circular epipolar light-field structure creates a simple sinusoidal relation between the objects of the scene and their curves in the epipolar image, opening the way of efficient reconstruction of circular light-fields.**

***Index Terms*—light-field, capture configuration, camera array**

I. Introduction

At the time of this paper, light-field capture and visualization technologies have already emerged to utilization in the industry, and the upcoming years of scientific effort in the area shall also enable efficient and cost-effective commercial use cases for individuals. Regarding visualization, the current state-of-the-art display systems support the glasses-free 3D experience in a horizontal parallax only (HPO) manner, which means that observer movement along the horizontal axis of physical reality creates the perception of a life-like parallax effect, but the same does not apply to the vertical axis. Approached from the perspective of use cases (e.g., public exhibition of a static or interactive light-field content), HPO visualization can fully serve its purpose, although the long-term aim of light-field visualization is to provide the full parallax that is perceivable in real life.

In a way, this concept is reflected in multi-camera light-field capture as well; the layout of many capture systems do not have a variation along the vertical axis, although there are indeed several solution for camera arrays which support full parallax capture. Within the scope of this paper, the introduced and investigated capture systems primarily neglect vertical layouts, yet it needs to be noted that the presented solutions are definitely applicable to such.

In "2D" HPO layouts of multi-camera light-field capture systems – where "2D" refers to the lack of vertical variation of camera positions – the most common practice is to use linear camera arrays. Such systems are called linear, because the components of the camera array are placed along either a single straight line, or along joint multiple straight lines. However, even though these are the most frequently used, they suffer from certain limitations and disadvantages compared to circular arrays, in which as the name indicates, cameras target the scene from a given arc.

In this paper, we provide an exhaustive analysis of light-fields captured by circular camera arrays, detail their potentials and limitations, and propose their usage for light-field reconstruction in particular. The research question investigated in this paper addresses the choice of linear and circular camera arrays for given use case scenarios. The paper highlights the benefits of the efficient usage of circular camera arrays and focuses on the differences with respect to linear camera arrays.

The remainder of the paper is structured as follows: Section II provides a brief overview of the available light-field capture systems. Section III introduces the relevant use cases. Section IV analyzes light-fields captured by circular camera arrays and examines their potential for light-field reconstruction. Section V provides a discussion about trends in research and development of the investigated area. The paper is concluded in Section VI.

II. Light-field capture systems

Light-field capture systems have come a long way since Lippmann's lens array based integral imaging technique in 1908 [1], but the basic concept remained the same: light-field can be captured by fusing together 2D images taken from different locations. This can be achieved by using portions of the same image sensor to capture images coming from different directions, or by using separate cameras at different positions. Both categories have modern light-field capture system implementations as seen on Fig. 1. For the purposes of this paper, however, the distinction based on baseline is more important. Baseline is defined by distance between the farthest view positions captured. In hand-held light-field cameras this is in the order of centimeters, while camera arrays typically have many cameras along a few meters of baseline, but small camera array systems also exist, such as the PiCam. In this paper we focus on light-fields captured by wide baseline systems of full size camera arrays.

The research in this paper was done as a part of and was funded from the European Unions Horizon 2020 research and innovation program under the Marie Sklodowska-Curie grant agreement No 676401, ETN-FPI, and No 643072, Network QoE-Net.

ISBN 978-90-827970-1-5 © EURASIP 2018

(a) Lytro light-field camera [2]

(b) Raytrix light-field camera [3]

(c) 2D array PiCam [4]

(d) Cameras in an arc [5]

Fig. 1. Light-field capture systems.

III. Use cases

As it was stated earlier, light-field visualization technologies are currently focused on industrial use cases. Such potential utilizations of these emerging systems include gas and oil exploration, industrial design, medical applications, air traffic control, ground and air vehicle head-up displays, military training, simulation, navigation and planning, and many more. The usage of light-field capture and display systems supports a higher level of accuracy at both ends, provides access to the visualized content to a large number of viewers simultaneously, performs well in interactive scenarios [6] and eliminates the need for additional viewing gears and devices.

Regarding what a future consumer market could hold for the users, one of the most promising application could be the so-called telepresence. Its greatest added value originates from the sense of presence, as light-field displays can show a real-time, glasses-free 3D visualization of the participant(s) of the call. For entertainment, beyond multimedia contents (i.e., real-time light-field video streaming [7]), gaming has an immense potential. More on mass entertainment, large-scale exhibitions and even cinema systems [8] are also promising. Furthermore, the technology has also great potential for education and training in general.

It needs to be noted that light-field displays may be configured for angular-selective utilization. This means that the field of view of the display may accommodate multiple contents and services simultaneously. For example, this scenario may be a multiplayer computer game, that shows the different game views to the different player in defined angle intervals.

IV. Light-fields of Camera Arrays

In this section, we illustrate real light-field data by the Blender render program using the "Volume emission 27" test scene from the demo files provided by the Blender foundation in Demo_274.zip [9].

A. Linear light-fields

Light-field processing traditionally has been done on planar and linear data structures. The first modern light-field format

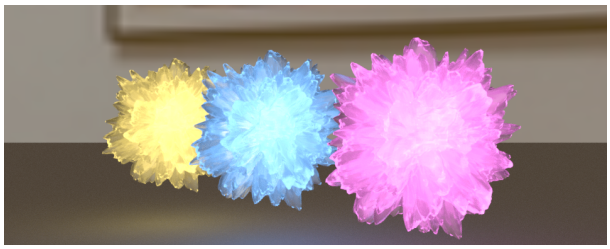

Fig. 2. Test scene: "Volume emission 27" scene from the Blender demo files.

defined the 4D light-field as rays intersecting two parallel planes [10]. One of the most commonly used capture setups of light-field is a linear camera array. Consequently many operations and processing algorithms were created that operate on data-sets captured by such linear camera systems [11] [12]. The most commonly used dense and linear light-field data structure is the epipolar plane image. The epipolar plane image is created by equidistant cameras facing the same direction on a camera line, then the images taken by the cameras are compiled in geometric order to a volume. The slices of this volume that are perpendicular to the original camera images are called the epipolar plane image (EPI) [13]. A special feature of the EPI is that objects of the scene are transformed into straight lines, whose slope indicates the depth and its origin indicates the horizontal position of the objects. Many algorithms exploit this property for processing the light-field [14] [15]. The EPI of our test scene is shown on Fig. 3, where the purple-pink object is observed to be in the foreground due to its highly inclined lines in the EPI.

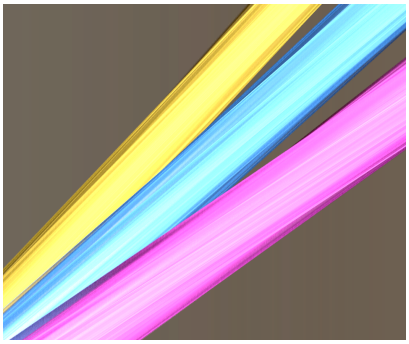

Fig. 3. Linear camera array epipolar image of the test scene indicating the three objects at different depths.

A clear advantage of using circular camera arrays is that the scene is possibly visible from all sides. This can be emulated by multiple linear camera array arrangements of course, but the resulting data-sets exist in their own frames of reference. Merging the data-sets from multiple linear camera array in order to facilitate their joint processing is a notable challenge, as the rays from one data-set intersect the camera line of the other data-sets only by chance. A full parallax camera array would solve this issue by ensuring a high degree of compatibility between rays of separate data-sets, but the

ISBN 978-90-827970-1-5 © EURASIP 2018

required amount of cameras makes this solution infeasible and is out of scope of this paper.

In case of HPO systems, the only common point between two linear camera arrays is the intersection point of the two camera lines, provided that it exists. Fig 4 illustrates a scenario in 2D where such common point exists. A camera placed to this point participates in both arrays, thus provides a limited possibility of joint processing. A common and prized problem with light-field camera arrays is the dense light-field reconstruction from sparse samples. The light-field captured by two sparse linear camera arrays could be jointly reconstructed by treating their common intersection point as a boundary condition, where the two linear datasets have a matching perspective of the scene. However, the full joint reconstruction would be the preferred solution.

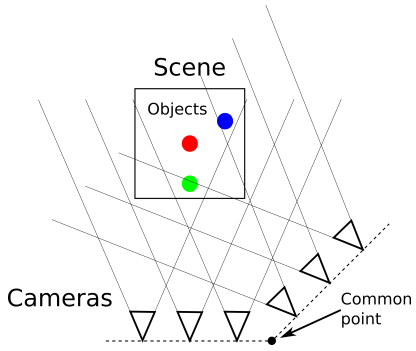

Fig. 4. Linear light-field capture setup with two camera segments. The red, green and blue dots represent the different objects within the scene.

B. Circular light-fields

In the circular camera array case, cameras from all sides are inherently in the common frame of reference as shown on Fig. 5. Even if the geometry of the scene does not allow a full circle array to surround the scene, cameras on a partial arc are able to capture the scene. The sole disadvantage of this scenario is the relatively fewer processing algorithms compared to the popular linear camera array case. We can define a circular EPI image analogous to the linear case by compiling the camera images in order of camera positions on the circle. Fig. 6 shows the circular EPI image of the test scene, indicating the blue object in the center of the circular camera array, and the two other objects next to it. The curves of the circular EPI are governed by Eq. 1, where a, b, c are constants calculable from the properties of the cameras and the capture geometry, $\mathbf{r}, \boldsymbol{\phi}$ are the polar coordinates of the object, α is the angle on the circle to the position of the camera, and y is the vertical coordinate of the object in the circular EPI. Observing the curve of an object from different views (α) at different positions in the image (y) allows us to fit this curve resulting in the position of the object in the scene in polar coordinates. This operation is possible [16], but due to the complicated relation, the fitting is impractical. It is important to note here that the circular light-field approach retains the property that the maximal slope of the curves in the circular EPI is related to the depth of the objects, thus the background and foreground objects can be separated as shown by Yucer *et al.* [17], as seen also on Fig. 6.

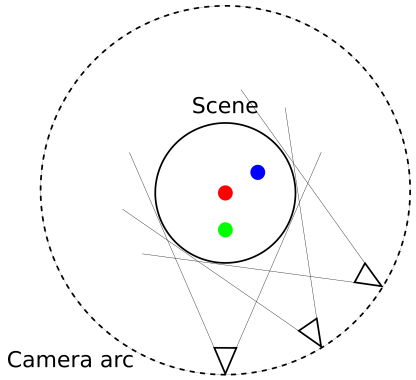

Fig. 5. Circular light-field capturing setup.

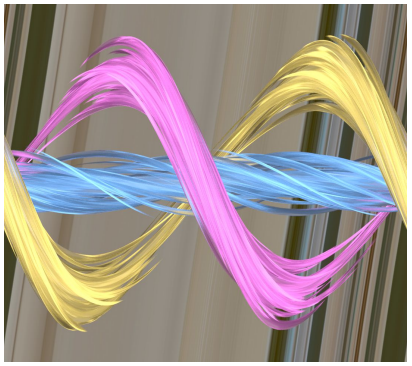

Fig. 6. Circular camera array epipolar image of the test scene.

$$y = \frac{a \cdot \mathbf{r} \cdot \cos(b \cdot \alpha + \boldsymbol{\phi})}{\mathbf{r} + c \cdot \sin(b \cdot \alpha + \boldsymbol{\phi})} \tag{1}$$

Our solution to the problem of complicated fitting of the circular light-field EPI curves is to use a different circular light-field structure. Instead of perspective cameras along the circular camera array, we propose to use cameras with spherical lenses, such that rays measured by these cameras are described by α, β, where α is the angle of the position of the camera, and β is angle of intersection between the measured ray and the circle as illustrated on Fig. 7. It may not be feasible to manufacture such an optical lens that provides this geometric quality to the camera system even in a limited field of view, but in this case, the image of an ordinary perspective camera can be resampled to provide the rays in the specified ray structure.

Using this α, β ray structure, objects in the scene are transformed also to curves illustrated on Fig.8. The black diagonal line is the invalid case, when $\alpha = \beta$ is true. Exploiting the periodical nature of the angles, the lower left triangle section can be translated to the other side of the

ISBN 978-90-827970-1-5 © EURASIP 2018

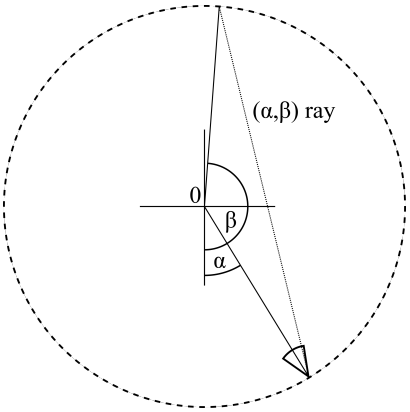

Fig. 7. Circular light-field indexing by ray origin (α) and destination (β).

upper right triangle section, thereby connecting the curves. Exploiting further periodic translations and applying a 45-degree coordinate transformation, we get the result shown on Fig. 9. In this α', β' coordinate frame the previously difficult curves turn into a simple sinusoidal function. The curves are described by Eq. 2, where a, b are constants calculable from the camera and the geometry, and $\mathbf{r}, \boldsymbol{\phi}$ are the polar coordinates of the object. This equation allows us to use this data structure to solve the light-field reconstruction problem by using convolutions and frequency analysis. However, due to this 45-degree coordinate transformation, the sampling lines of a camera are also transformed or rotated as illustrated on Fig. 10, where vertical exclusions zones due to the finite field of view of cameras, and diagonal exclusions zones from a 120-degree camera arc are also shown.

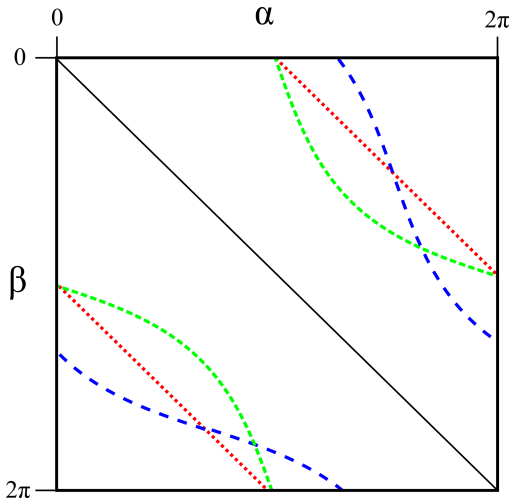

Fig. 8. Circular EPI in α and β coordinates. The red, green and blue lines represent the different objects within the scene, introduced in prior figures.

$$\beta' = a \cdot \mathbf{r} \cdot \cos(b \cdot \alpha' + \boldsymbol{\phi}) \tag{2}$$

Our test scene is shown in the α, β coordinate frame on Fig. 11 and the perfect sines on Fig. 12 in the novel α', β'

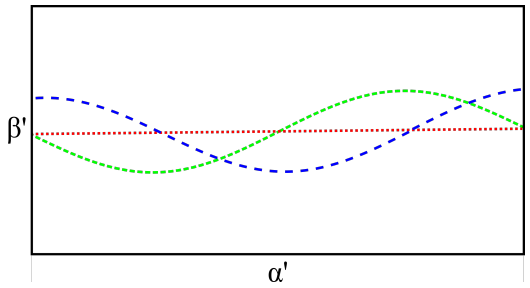

Fig. 9. Circular EPI after coordinate transformation and translation.

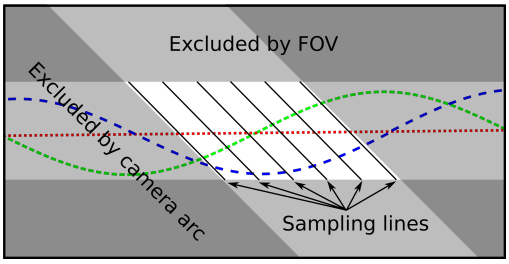

Fig. 10. Available circular EPI samples with 6 cameras on a 120° arc.

transformed coordinate frame. As shown before, in a realistic scenario only a portion of this data-set would be captured due to the limited field of view, camera arc and finite amount cameras, but these are challenges analogous to the linear camera array case, where they have already had been overcome in real scenarios [18]. The sole difference is that due to the sines instead of straight lines, a different frequency analysis method is required to reconstruct the dense light-field from the available samples.

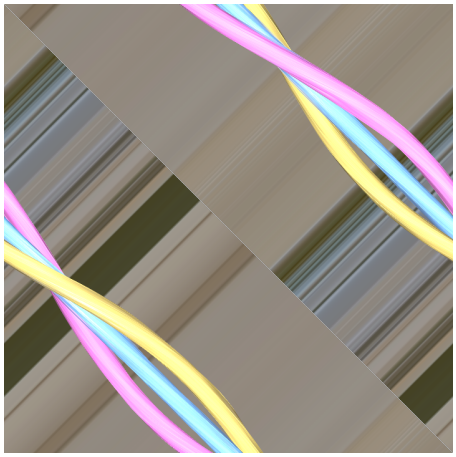

Fig. 11. Circular EPI of the test scene in α,β coordinates.

V. Discussion

It is clear that linear camera array systems are less complicated from both the mechanical and the processing point of view, and the calibration of circular capture systems is

ISBN 978-90-827970-1-5 © EURASIP 2018

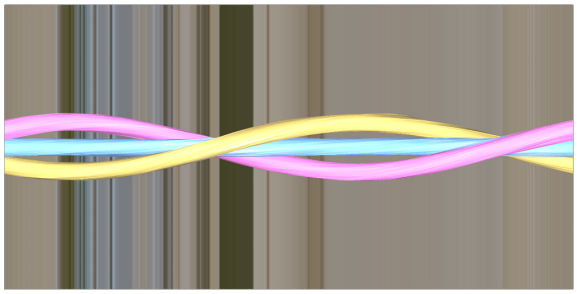

Fig. 12. Test scene circular EPI after coordinate transformation.

more challenging. However, our conclusion stands that circular capture systems and data structures allow the seamless integration of light-field information from many sides of the scene, even if the camera arc is limited by geometric factors. The resampled circular light-field presented in this paper reduces the processing challenges of further work about circular light-fields, and can be useful for many light-field capturing use cases.

Regarding such use cases, circular light-field capture does not necessarily limit utilization, yet there are certain considerations for implementation that must not be overlooked. First of all, single-camera systems are perfectly viable, if the content to be captured is a static scene, and the camera moves along the defined arc. For real-time use cases such as telepresence, using a smaller portion of the camera arc can be sufficient, and thus can be implemented with a limited number of cameras, although a high-end multi-participant conferencing system may benefit from a full arc. Medical imaging also favors a full camera arc, yet there can be a lesser requirement for real-time capabilities.

As for future research, the great utilization potentials come with the need for great scientific effort. One of the biggest challenges is to create full light-field reconstruction itself for circular light-fields, which in the more straightforward case of linear light-field already posed significant difficulties. Also, for the quality evaluation and performance assessment of such methods, light-field displays are required, which are commercially available, yet demand a rather high cost, and thus limits the number of institutions that can obtain access to such visualization technology.

VI. Conclusions

In this paper, we presented common HPO light-field data structures and capture methods used by the research community. We analyzed their advantages and disadvantages focusing on the problem of light-field reconstruction, and their ability to collect information from more than one side of the scene. The main contribution of this paper is the novel circular EPI space, that provides a simple sinusoidal relation between the location of objects and their curve in the EPI space.

As future work, we will research the possible convolutions and basis functions in frequency space that can efficiently transform this novel circular EPI image to a data structure, where a high-quality and efficient light-field reconstruction can be performed. We foresee that direct strategies, such as voxel based search in image space for corresponding sines in this circular EPI space will result in inefficient algorithms both in terms of quality and computing time.

References

[1] G. Lippmann, "Epreuves reversibles. photographies integrals," *Comptes-Rendus Academie des Sciences*, vol. 146, pp. 446–451, 1908.

[2] C. Sung, "Lytro light field camera," White Paper https://christinesung.files.wordpress.com/2014/01/lytrowhitepaper.pdf (retrieved Feb. 2018).

[3] C. Perwass and L. Wietzke, "Single lens 3D-camera with extended depth-of-field," in *IS&T/SPIE Electronic Imaging*. International Society for Optics and Photonics, 2012.

[4] K. Venkataraman, D. Lelescu, J. Duparré, A. McMahon, G. Molina, P. Chatterjee, R. Mullis, and S. Nayar, "PiCam: An ultra-thin high performance monolithic camera array," *ACM Transactions on Graphics (TOG)*, vol. 32, no. 6, 2013.

[5] M. Tanimoto, M. P. Tehrani, T. Fujii, and T. Yendo, "Free-viewpoint TV," *IEEE Signal Processing Magazine*, vol. 28, no. 1, pp. 67–76, 2011.

[6] V. K. Adhikarla, J. Sodnik, P. Szolgay, and G. Jakus, "Exploring direct 3D interaction for full horizontal parallax light field displays using leap motion controller," *Sensors*, vol. 15, no. 4, pp. 8642–8663, 2015.

[7] P. A. Kara, A. Cserkaszky, M. G. Martini, A. Barsi, L. Bokor, and T. Balogh, "Evaluation of the Concept of Dynamic Adaptive Streaming of Light Field Video," *IEEE Transactions on Broadcasting*, vol. 64, no. 2, pp. 407–421, 2018.

[8] P. A. Kara, Z. Nagy, M. G. Martini, and A. Barsi, "Cinema as large as life: Large-scale light field cinema system," in *3D Immersion (IC3D), 2017 International Conference on*. IEEE, 2017.

[9] Blender, "Volume emission 27 demo scene," https://download.blender.org/demo/test/Demo_274.zip (retrieved Feb. 2018).

[10] M. Levoy and P. Hanrahan, "Light field rendering," in *Proceedings of the 23rd annual conference on Computer graphics and interactive techniques*. ACM, 1996, pp. 31–42.

[11] W. Matusik and H. Pfister, "3D TV: a scalable system for real-time acquisition, transmission, and autostereoscopic display of dynamic scenes," in *ACM Transactions on Graphics (TOG)*, vol. 23, no. 3. ACM, 2004, pp. 814–824.

[12] B. Wilburn, N. Joshi, V. Vaish, E.-V. Talvala, E. Antunez, A. Barth, A. Adams, M. Horowitz, and M. Levoy, "High performance imaging using large camera arrays," in *ACM Transactions on Graphics (TOG)*, vol. 24, no. 3. ACM, 2005, pp. 765–776.

[13] R. C. Bolles, H. H. Baker, and D. H. Marimont, "Epipolar-plane image analysis: An approach to determining structure from motion," *International journal of computer vision*, vol. 1, no. 1, pp. 7–55, 1987.

[14] M. W. Tao, S. Hadap, J. Malik, and R. Ramamoorthi, "Depth from combining defocus and correspondence using light-field cameras," in *Computer Vision (ICCV), 2013 IEEE International Conference on*. IEEE, 2013, pp. 673–680.

[15] S. Vagharshakyan, R. Bregovic, and A. Gotchev, "Image based rendering technique via sparse representation in shearlet domain," in *Image Processing (ICIP), 2015 IEEE International Conference on*. IEEE, 2015, pp. 1379–1383.

[16] I. Feldmann, P. Eisert, and P. Kauff, "Extension of epipolar image analysis to circular camera movements," in *Image Processing, 2003. ICIP 2003. Proceedings. 2003 International Conference on*, vol. 3. IEEE, 2003.

[17] K. Yücer, A. Sorkine-Hornung, O. Wang, and O. Sorkine-Hornung, "Efficient 3D object segmentation from densely sampled light fields with applications to 3D reconstruction," *ACM Transactions on Graphics (TOG)*, vol. 35, no. 3, 2016.

[18] S. Vagharshakyan, R. Bregovic, and A. Gotchev, "Light field reconstruction using shearlet transform," *IEEE transactions on pattern analysis and machine intelligence*, vol. 40, no. 1, pp. 133–147, 2018.

ISBN 978-90-827970-1-5 © EURASIP 2018